Enhancement of superconductivity in the Fibonacci chain

Meng Sun [1,2,*] Tilen Čadež [2] Igor Yurkevich [3,2] and Alexei Andreanov [2,4,†]

[1]*School of Physics and Optoelectronic Engineering, Beijing University of Technology, Beijing 100124, China*
[2]*Center for Theoretical Physics of Complex Systems, Institute for Basic Science, Daejeon 34126, Republic of Korea*
[3]*School of Computer Science and Digital Technologies, Aston University, Birmingham B4 7ET, United Kingdom*
[4]*Basic Science Program, Korea University of Science and Technology, Daejeon 34113, Republic of Korea*

(Received 11 July 2023; revised 2 February 2024; accepted 4 March 2024; published 2 April 2024)

We study the interplay between quasiperiodic disorder and superconductivity in a one-dimensional tight-binding model with the quasiperiodic modulation of on-site energies that follow the Fibonacci rule, and all the eigenstates are multifractal. As a signature of multifractality, we observe the power-law dependence of the correlation between different single-particle eigenstates as a function of their energy difference. We numerically compute the mean-field superconducting transition temperature for every realization of a Fibonacci chain of a given size and find the distribution of critical temperatures, analyze their statistics, and estimate the mean value and variance of critical temperatures for various regimes of the attractive coupling strength and quasiperiodic disorder. We find an enhancement of the critical temperature compared to the analytical results that are based on strong assumptions of the absence of correlations and self-averaging of multiple characteristics of the system, which are not justified for the Fibonacci chain. For the very weak coupling regime, we observe a crossover where the self-averaging of the critical temperature breaks down completely and strong sample-to-sample fluctuations emerge.

DOI: 10.1103/PhysRevB.109.134504

I. INTRODUCTION

Fractals are intricate geometric objects that are self-similar across different scales [1,2]. The concept of fractality has revolutionized the development of novel materials and devices, offering unique properties and applications. Materials featuring fractal structures showcase exceptional characteristics typically not observed in their nonfractal counterparts. One remarkable example is the recent advancement in fractal graphene-based materials [3]. These materials display remarkable mechanical strength, electrical conductivity, and thermal stability, making them highly suitable for a diverse range of applications, including energy storage and sensing. The fractal structures have proven to be efficient in photovoltaic devices [4] since they enhance light absorption and significantly improve the efficiency of solar cells. For instance, the utilization of fractal-shaped nanowires in solar cells has led to heightened light trapping and absorption compared to conventional designs [5].

From a theoretical perspective, there have been notable efforts to explore the conditions under which fractal geometry can enhance a property critical for applications, such as superconductivity. Following the development of the microscopic theory of superconductivity by Bardeen, Cooper, and Schrieffer (BCS) [6–8], the influence of disorder on superconductivity garnered considerable attention [9–15]. Early studies [16–19] suggested that a superconducting phase could emerge when the Fermi energy E_F resides in the region of the Anderson mobility edge due to strong correlations between fractal wave functions. Subsequent research predicted an increase in critical temperature even in quasi-one-dimensional (quasi-1D) wires [20–22], quasi-two-dimensional (quasi-2D) materials [19], and weakly disordered 2D systems [23].

While many studies (see Refs. [17,18,24,25] and references therein) focused on the situation when the transition in a clean system described by the standard BCS-type mean-field theory is modified by disorder, inducing significant overlap between multifractal wave functions with different eigenenergies, there are also quasiperiodic materials that possess these features intrinsically without extrinsic disorder [26,27]. Quasiperiodic systems, readily realized experimentally in various structures like artificial atomic chains and quasi-2D semiconducting heterostructures [28], serve as examples. The Fibonacci chain [29–33], a one-dimensional quasiperiodic structure closely related to three-dimensional icosahedral quasicrystals [34,35], offers an intriguing realm for superconductivity studies. The energy spectrum in this system exhibits a Cantor-set-type fractal structure [36], and the multifractal eigenfunctions demonstrate long-range power-law spatial and temporal correlations. It is therefore a natural test bed for the effect of fractality on the superconducting properties.

Phenomenological arguments were put forward [25] suggesting multifractal correlations of wave functions enhance superconductivity. This was later tested close to the Anderson transition within a mean-field approximation [18]. The difficulty is that in this setting one has to solve a disordered gap equation without the simplifications brought in by translation invariance. A common approach is to average the gap

*msun_89@bjut.edu.cn
†aalexei@ibs.re.kr

equation and ignore the correlations [19]. As we demonstrate in this work, neglecting the correlations removes an important enhancement of the critical temperature.

The outline of this paper is as follows. We define the model and study its spectral correlation function in Sec. II. Then the mean-field approximation of superconductivity in the model and the behavior of the average critical temperature are studied in Sec. III. The breakdown of self-averaging of the critical temperature and the crossover in the coupling strength are discussed in Sec. IV, followed by conclusions in Sec. V.

II. MODEL AND SPECTRAL CORRELATION FUNCTION

We consider the 1D Fibonacci chain, which serves as a fundamental model representing quasicrystals. This chain exhibits several noteworthy properties, as outlined in a recent study by Jagannathan [29]: (1) deterministic construction, (2) a finite number of possible configurations for chains of finite length, and (3) multifractal eigenstates. The Fibonacci chain is constructed following a well-defined deterministic algorithm. Despite its complexity, the Fibonacci chain possesses a finite number of possible configurations, allowing detailed analysis. Finally, one of the remarkable features of the Fibonacci chain is that its eigenstates exhibit multifractal behavior for all strengths of the on-site potential h, leading to intricate patterns with varying degrees of complexity and self-similarity, regardless of the specific values of the on-site potential.

Here we focus on a chain model with on-site energies arranged according to the Fibonacci rule. The tight-binding Hamiltonian,

$$\hat{H}_F = -\sum_i (\hat{c}_i^\dagger \hat{c}_{i+1} + \hat{c}_{i+1}^\dagger \hat{c}_i + h_i \hat{c}_i^\dagger \hat{c}_i), \tag{1}$$

describes particles hopping between lattice sites with dimensionless (measured in units of hopping amplitude) on-site potential h_i. The potential takes two values $\pm h$, which are arranged according to the Fibonacci sequence rule $\mathcal{F} : \{A \to AB, B \to A\}$. The nth Fibonacci sequence S_n is the concatenation of the two previous ones $S_n = [S_{n-1}, S_{n-2}]$. To construct the Fibonacci-type potential for a system of size L, we first write down a long enough Fibonacci sequence, then cut a segment containing L consecutive letters, and make the substitution $A \to h$ and $B \to -h$. The number of different segments is $N = L/2$ [$N = (L-1)/2$] for even (odd) L [30]. In this way, we generate an ensemble of N different realizations of on-site energy arrangements, each being a subset of the Fibonacci sequence.

Some properties of the eigenstates of the Fibonacci chain were studied recently [29,37,38]. For example, a perturbative renormalization group analysis was used to analytically determine fractal dimensions for the off-diagonal Fibonacci chain [32] in the weak potential strength limit ($h \ll 1$).

For the issue of superconducting transition, the most important property of multifractal systems [17,25] is the energy-resolved overlap of different eigenstates described by the correlation of two single-particle wave functions [25],

$$C(\omega) = L^d \sum_{\mathbf{r},n,m} \langle |\psi_n(\mathbf{r})|^2 |\psi_m(\mathbf{r})|^2 \delta(\epsilon_m - \epsilon_n - \omega) \rangle, \tag{2}$$

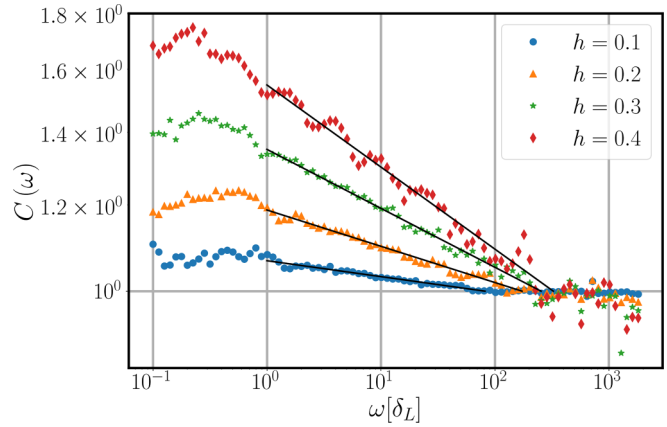

FIG. 1. The correlation function (3) of the Fibonacci chain for fixed system size $L = 2000$ and several disorder strengths. The solid black lines are the power-law fits, Eq. (3). The fitted values of γ and E_0 are $\gamma \sim 0.0146, 0.0333, 0.0542, 0.0754$ and $E_0 \sim 82.1, 173.3, 254.6, 325.9[\delta_L]$ for $h = 0.1, 0.2, 0.3, 0.4$.

where L^d is the system volume, $\psi_n(\mathbf{r})$ and ϵ_n are the eigenstate and eigenenergy of the Hamiltonian (1), respectively, and ω is the fixed energy difference between two eigenstates. This function demonstrates power-law decay at the Anderson transition [17,39],

$$C(\omega) = \left(\frac{E_0}{|\omega|}\right)^\gamma, \tag{3}$$

in some frequency domain $\delta_L < \omega < E_0$, where δ_L is the mean level spacing and E_0 is the energy scale. The power-law exponent γ is connected to the multifractal dimension by the simple relation [18,25,40] $\gamma = 1 - \frac{d_2}{d}$, where d is the spatial dimension of the system and d_2 is the fractal dimension of eigenfunctions [41].

We confirm the power-law decay of the correlation in the Fibonacci chain (see Fig. 1) for different disorder strengths by numerical diagonalization of the Hamiltonian (1) and averaging over different realizations, i.e., different slices of the length L cut from the nth Fibonacci word. Using the numerically computed correlator (3), we further estimate the upper energy scale E_0 and the exponent γ from the power-law fits shown in Fig. 1. Similar behavior of correlation functions was also confirmed in Ref. [42]. We also note that in a recent work [43], Jagannathan and Tarzia focused on the disorder effects on the quasiperiodic tiling, and they observed the nonmonotonic evolution of spatial properties of eigenstates with disorder strength but only as a finite-size effect vanishing in the thermodynamic limit. However, in this work, we study modifications present in long, but finite, chains.

III. MEAN-FIELD SUPERCONDUCTIVITY

The spinful fermions on a tight-binding chain with local attraction are described by the negative-U Hubbard Hamiltonian,

$$\hat{H} = \sum_\sigma \hat{H}_{F,\sigma} + U \sum_{i=1}^{L} \hat{n}_{i\uparrow} \hat{n}_{i\downarrow}, \tag{4}$$

where the single-particle part $\hat{H}_{F,\sigma}$ is given by Eq. (1) for each of the spin components $\sigma = \uparrow, \downarrow$. The second term, with $\hat{n}_{i\sigma} = \hat{c}^{\dagger}_{i\sigma}\hat{c}_{i\sigma}$ being the occupation number operator of electrons with spin σ on the ith site, is the attractive Hubbard interaction with dimensional coupling constant U.

To investigate the superconducting properties we write the Hamiltonian in the single-particle eigenbasis of $\hat{H}_{F,\sigma}$,

$$\hat{c}_{i\sigma} = \sum_{n} \psi_n(i)\, \hat{c}_{n\sigma}, \tag{5}$$

following [17,44] and keep only the terms most relevant for the superconductivity:

$$\hat{H} = \sum_{n\sigma} \epsilon_n \hat{c}^{\dagger}_{n\sigma}\hat{c}_{n\sigma} + U \sum_{nm} M_{nm}\hat{c}^{\dagger}_{n\uparrow}\hat{c}^{\dagger}_{n\downarrow}\hat{c}_{m\uparrow}\hat{c}_{m\downarrow}, \tag{6}$$

$$M_{nm} = \sum_{i} |\psi_n(i)|^2 |\psi_m(i)|^2, \tag{7}$$

where ϵ_n is the single-particle energy of eigenstate n obtained from Eq. (1) and $\sigma = \{\downarrow, \uparrow\}$ is the spin label. The subscripts n and m label the eigenvalues and eigenstate, and the index i is the lattice index. The mean-field approach [45] leads to the gap equation

$$\Delta_n = \frac{|U|}{2} \sum_{m} \frac{M_{nm}\Delta_m}{\varepsilon_m} \tanh\left(\frac{\epsilon_m}{2T}\right), \tag{8}$$

where $\varepsilon_m = \sqrt{\epsilon_m^2 + \Delta_m^2}$ is the excitation energy of the superconductor [45] and the gap function is defined as an anomalous Green's function, $\Delta_n = \langle \hat{c}_{n\uparrow}\hat{c}_{n\downarrow}\rangle$. The superconducting transition is signaled by the appearance of a nonzero Δ_n with changing temperature T.

The routine approach to analyzing the transition is based on a few assumptions [17–19]:

(1) The density of states and the wave functions are uncorrelated.

(2) The density of states ν_0 is self-averaging and energy independent in the window of the Debye frequency ϵ_D around the Fermi energy, for example, one assumes the phonon-electron interaction, which, after elimination of phonons, can be presented as a pointlike attraction (similar to the attractive Hubbard term) but only between electrons whose energies are within the Debye energy width window around the Fermi level. This is a standard assumption leading to the so-called BCS theory with effective Hubbard-like energy-dependent attraction $U(\epsilon)$,

$$U(\epsilon) = \begin{cases} \lambda/\nu_0, & \epsilon < \epsilon_D, \\ 0, & \epsilon \geqslant \epsilon_D, \end{cases} \tag{9}$$

where ν_0 is the density of states at the Fermi level and λ is the dimensionless coupling constant.

(3) All gap functions Δ_n are self-averaging.

(4) Finally, there is no correlation between the wave functions' overlap integral M_{nm} and the gaps Δ_n.

Only under all the above-mentioned conditions does the gap equation acquire the following form in the continuous limit after averaging over the disorder realizations:

$$\Delta(\epsilon) = \frac{\lambda}{2} \int_{-\epsilon_D}^{\epsilon_D} \frac{d\epsilon'}{\varepsilon(\epsilon')} C(\epsilon - \epsilon') \tanh\left(\frac{\varepsilon(\epsilon')}{2T}\right) \Delta(\epsilon'). \tag{10}$$

Here the eigenenergies ϵ_n and ϵ_m of the Fibonacci chain are substituted with the continuous energies ϵ and ϵ' under the assumption that all other energy scales are much larger than the mean level spacing, and $\varepsilon(\epsilon')$ is the same excitation energy as defined after Eq. (8). Further assuming that all the gaps Δ_n vanish at the transition, i.e., in the continuous limit $\Delta(\epsilon) = 0$, and that the Debye energy ϵ_D is much larger than the fractal scale E_0 leads to the following equation for the critical temperature:

$$1 = \lambda \int_{0}^{\epsilon_D} \frac{C(\epsilon)}{\epsilon} \tanh\left(\frac{\epsilon}{2T_c^A}\right) d\epsilon, \tag{11}$$

which admits the solution

$$T_c^A = \epsilon_D \mathcal{D}(\gamma) \left[1 + \frac{\gamma}{\lambda}\left(\frac{\epsilon_D}{E_0}\right)^{\gamma}\right]^{-\frac{1}{\gamma}}, \tag{12}$$

with

$$\mathcal{D}(\gamma) = [2\gamma(2^{\gamma+1} - 1)\Gamma(-\gamma)\zeta(-\gamma)]^{\frac{1}{\gamma}}, \tag{13}$$

where $\zeta(x)$ is the Riemann ζ function [19].

We extract the values of E_0 and γ from the correlation function (2), which takes the power-law scaling form (3), as we verified in Sec. II. With these averaged parameters, we can evaluate the critical temperature using Eq. (12). We show in Fig. 2 by the solid line the critical temperature computed via Eq. (12) as a function of the coupling strength for the Fibonacci chain system with different potential strengths.

However, this approach is based on at least four assumptions outlined above which are hard to justify. Instead, we compute the critical temperature numerically without *a priori* assumptions on statistics and correlations between various entries present in Eq. (8). We solve the linearized gap equation (8) in the limit of vanishing gaps $\Delta_n \to 0$,

$$\Delta_n = \frac{\lambda}{2\nu_0} \sum_{m}^{|\epsilon_m| < \epsilon_D} \frac{M_{nm}}{\epsilon_m} \tanh\left(\frac{\epsilon_m}{2T_c}\right) \Delta_m, \tag{14}$$

to find the critical temperature T_c numerically for every realization of the Fibonacci potential and then analyze the statistics of the ensemble of critical temperatures: their distribution function, mean value, and variance.

The results for the average critical temperature of the Fibonacci chain, computed along the above lines, are presented in Fig. 2 for several system sizes L, disorder strengths h, and couplings λ. For the convenience of presentation, the points are manually shifted horizontally for fixed couplings λ. The vertical bars show the standard deviation of the critical temperature. For convenience we show the error bars only for the case $h = 0.30$; the error bars for other disorder strengths show similar behavior. Finally, we estimate the critical temperature in the thermodynamic limit using the finite-size extrapolation. The results are shown by black markers.

We observe that over a wide range of couplings the average critical temperature is self-averaging with small variance. The variance increases significantly as the coupling strength is decreased, as seen in the bottom plot of Fig. 2. This suggests the existence of a crossover coupling strength $\tilde{\lambda}$ below which the critical temperature starts to lose its self-averaging property and sample-to-sample fluctuations become important.

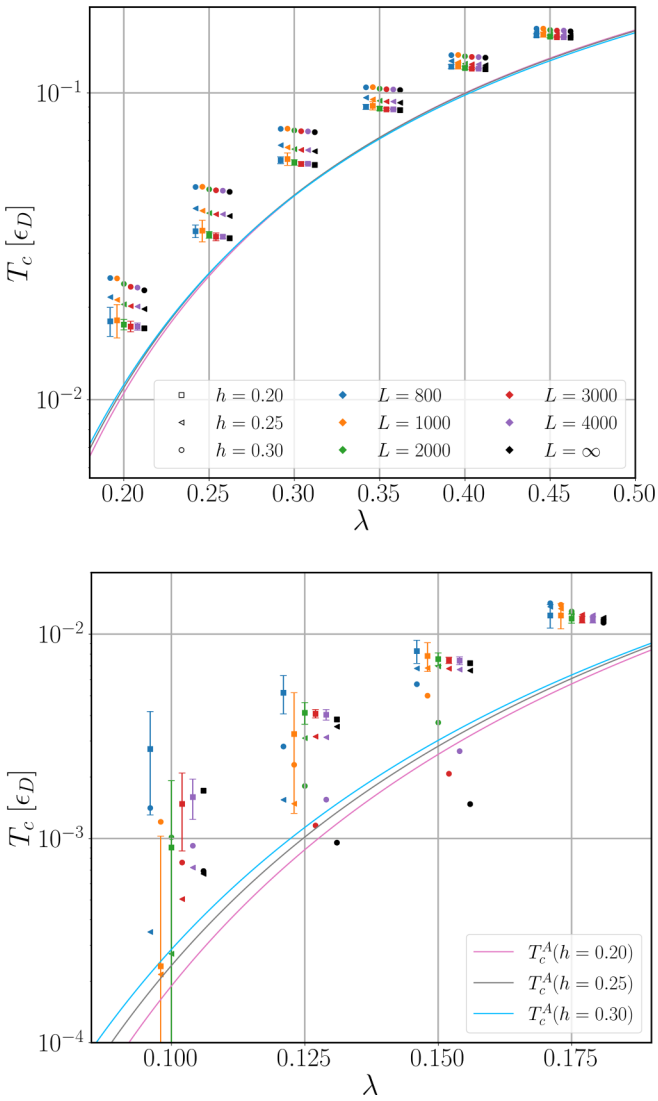

FIG. 2. Average critical temperature for different system sizes (shown by the color of the markers) and different disorder strengths (shown by the shape of the markers). The black points are the result of the extrapolation to the infinite size. The solid lines are the analytical result of Ref. [19] given by Eq. (12). The vertical bars show the temperature variance for disorder $h = 0.3$. For different system sizes and disorder strengths, the markers are shifted to the left and right relative to the green markers. Top: larger couplings λ. Bottom: small couplings λ.

A detailed discussion of this crossover and its properties is provided in the next section.

The main result shown in Fig. 2 is the clear discrepancy between the two procedures: assuming self-averaging properties and the absence of correlation followed by analytic solution of the Eq. (12) and a straightforward numerical analysis of random critical temperatures found from the nonaveraged Eq. (14) with no assumptions at all. That is, although the critical temperature itself self-averages, this self-averaging value is different from the solution of Eq. (12). In most regions of the coupling strength, we find an enhancement of the critical temperature compared to the analytical formula, Eq. (14). We attribute this additional enhancement to the proper treatment

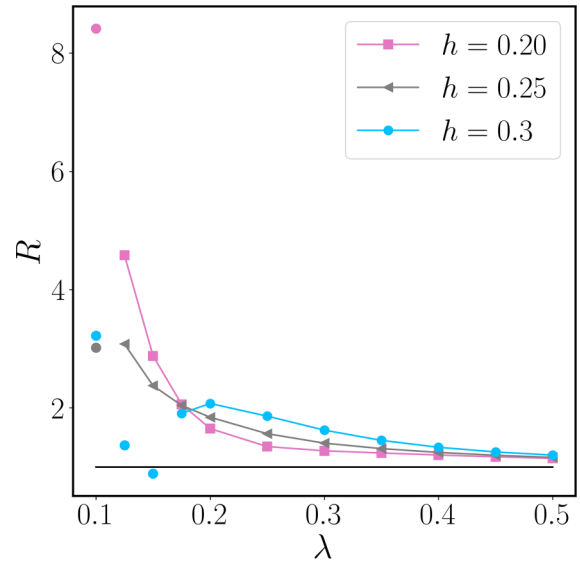

FIG. 3. The enhancement ratio $R = T_c^N/T_c^A$ vs coupling λ at $L = 4000$ for different disorder strengths h: 0.2 (squares), 0.25, (triangles) and 0.3 (circles). T_c^N is the critical temperature computed numerically; T_c^A is the critical temperature predicted by Ref. [19]. The markers are connected by solid lines in the region $\lambda > \tilde{\lambda}$. The black line corresponds to $R = 1$ and is shown for convenience.

of the Debye cutoff energy in our approach: as explained in the Appendix of Ref. [19], Mayoh and García-García's analytical expression is achieved by extending the integral limit of Eq. (11) from ϵ_D to infinity, which is not always justified for a power-law correlations between eigenstates. By denoting the average critical temperature following from Eq. (14) as T_c^N, we calculate the enhancement ratio $R = T_c^N/T_c^A$, as shown in Fig. 3. For visual convenience, the ratio data points are connected by lines for the coupling strengths above the self-averaging crossover, $\lambda \geqslant \tilde{\lambda}$. As one can see, the enhancement ratio is suppressed by increasing the coupling strength, and both results, Eqs. (12) and (14), converge to the mean-field theory. This behavior can be explained by the competition between the coupling λ and the disorder h. As $\lambda > h$, the coupling strength is dominant, and the formation of Cooper pairs is local, not affected by the realization of the disorder potential. On the other hand, when $\lambda < h$, the potential takes the main role in defining which state and its time-reversal partner are to be coupled. This results in a further enhancement in critical temperature due to the multifractality of wave functions and larger variance due to the sensitivity to disorder realization.

IV. BREAKDOWN OF SELF-AVERAGING AND CROSSOVER IN THE COUPLING STRENGTH

We saw in Fig. 2 that the variance of the average critical temperature increases significantly for small enough couplings λ. In this section, we discuss the breakdown of the self-averaging of the critical temperature and quantify the crossover coupling strength $\tilde{\lambda}$.

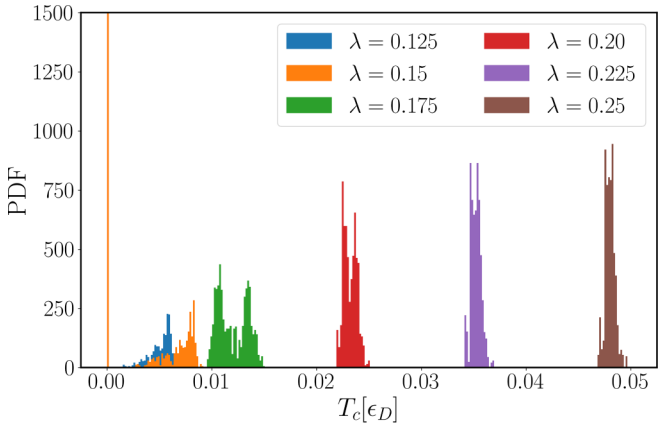

FIG. 4. The PDF of the critical temperatures for disorder strength $h = 0.3$ and $L = 4000$ for different coupling strengths. The crossover coupling strength is $\tilde{\lambda} \approx 0.16$.

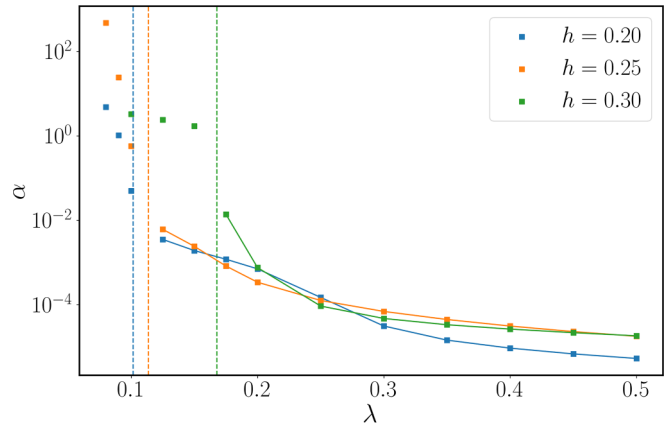

FIG. 5. The self-averaging metric α vs λ for different disorder strengths h at system size $L = 4000$. The vertical dashed lines denote the position of the crossover $\tilde{\lambda}$ for the respective disorder strengths. The points in the self-averaging regime, $\lambda > \tilde{\lambda}$, are connected by the solid lines. α becomes order 1 for $\lambda \lesssim \tilde{\lambda}$.

In order to define the crossover coupling strength $\tilde{\lambda}$, we use Eq. (14), from which we extract the critical temperature

$$\lambda W(T)\,\mathbf{\Delta} = \mathbf{\Delta}. \tag{15}$$

It is an eigenproblem equation for the matrix W with the following matrix elements:

$$W_{nk}(T) = \frac{M_{nk}}{2\nu_0\epsilon_k}\tanh\left(\frac{\epsilon_k}{2T}\right). \tag{16}$$

Note that W depends explicitly on the disorder realization through the eigenvalues ϵ_k and eigenstates of the Fibonacci chain appearing in M (7). It directly follows from the above equations that for a given realization of the Fibonacci potential, the superconducting instability at some finite T exists only if the largest eigenvalue $\Lambda(T = 0)$ of $W(T = 0)$ is greater than $1/\lambda$, or, equivalently, $\lambda \geqslant 1/\Lambda(T = 0)$. Based on this and the finite number of realizations of the Fibonacci potential for a given system size L, we define

$$\tilde{\lambda}^{-1} = \min_{\{h_i\}} \Lambda(T = 0), \tag{17}$$

where the min is taken over the realizations of the Fibonacci potential. The coupling $\tilde{\lambda}$ corresponds to the appearance of the first disorder realization without a superconducting phase.

We now demonstrate that $\tilde{\lambda}$ provides a proper definition of the crossover coupling, below which the self-averaging property of T_c is lost. The naive argument is as follows: for $\lambda < \tilde{\lambda}$ more and more disorder realizations stop having a superconducting phase, therefore increasing the sample to sample fluctuations and making the average less well defined. In Fig. 4, we show the probability density distributions (PDFs) of critical temperatures for several values of λ with $\tilde{\lambda} \approx 0.16$. We observe that as the coupling strength is decreased, the average T_c becomes less representative. For $\lambda > \tilde{\lambda}$, the PDF has a bell shape and can be reasonably well approximated by a Gaussian, for instance, at $\lambda = 0.25$. Closer to the crossover value $\tilde{\lambda}$, the distributions (green and red) spread out, and several close peaks appear in the PDF. For $\lambda < \tilde{\lambda}$, the distribution continues to spread and acquires a visible tail for smaller T_c, and the trivial case $T_c = 0$ starts to accumulate (orange and blue). As a consequence, the standard deviation of the critical temperature increases significantly.

To further investigate the crossover coupling strength and the breakdown of self-averaging of the critical temperatures, we study the following metric of self-averaging:

$$\alpha = \frac{\langle T_c^2\rangle}{\langle T_c\rangle^2} - 1, \tag{18}$$

which quantifies the fluctuations around the average compared to the average itself: it is zero for a perfectly self-averaging quantity (with δ-function distribution). The values of order 1 indicate that fluctuations around the average become comparable to the average itself, and the self-averaging property is lost. In Fig. 5, we show the values of α computed for the Fibonacci chain for different disorder strengths h at system size $L = 4000$. The vertical dashed lines indicate the position of the crossover $\tilde{\lambda}$ for several disorder strengths. The solid lines connect the points for couplings above the crossover $\tilde{\lambda}$. We observe from Fig. 5 that the two definitions of the crossover from self-averaging to no self-averaging, α and $\tilde{\lambda}$, agree well. The jump in the self-averaging parameter α from

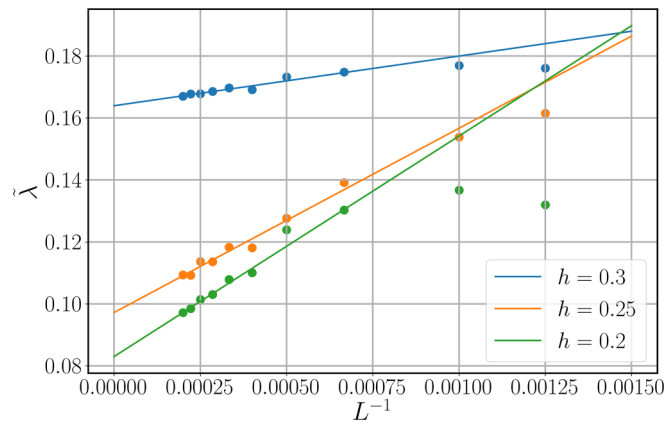

FIG. 6. Finite-size scaling for the crossover coupling $\tilde{\lambda}$ vs system size L. The fits are based on the data for the seven largest sizes: $L = 2000, 2500, 3000, 3500, 4000, 4500, 5000$.

values of order 10^{-2} to values of order 1 occurs precisely around the coupling $\tilde{\lambda}$.

Last, we extract the thermodynamic limit of $\tilde{\lambda}$ by extrapolation, as shown in Fig. 6: extrapolation suggests finite values of $\tilde{\lambda}$ in the thermodynamic limit. Also, the crossover $\tilde{\lambda}$ decreases with decreasing disorder strength. This behavior can be anticipated as follows: for $h = 0$, the system is described by the BCS theory and $T_c \sim \exp(-1/\lambda)$. For a finite disorder, the nonzero values of $\tilde{\lambda}$ indicate a transition from the superconducting phase to the insulator phase. The observed dependence of $\tilde{\lambda}$ on disorder strength naturally connects the two limits.

V. CONCLUSIONS

In this work, we considered an open 1D chain with the Fibonacci potential h and calculated correlation of two single-particle wave functions for different disorder strengths h. We found a power-law behavior of the correlation function, which reflects the multifractal character of the eigenstates of the Fibonacci chain. Using the single-particle eigenstates, we used the mean-field theory to compute the critical temperature of the superconducting transition following two different procedures: (1) averaging Eq. (14) first, then solving it for T_c, e.g., by averaging the spatial correlation function $C(\omega)$ and estimating the multifractal related parameters γ and E_0, we analytically calculated the critical temperature via Eq. (12) assuming self-averaging of all characteristic variables (as explained above); (2) we first solved Eq. (14) and then performed averaging, e.g., by solving Eq. (14) numerically for the critical temperature for a fixed realization of the Fibonacci potential and analyzing the statistics (PDF, mean value, and variance) of the ensemble of critical temperatures.

We found a clear discrepancy between the results obtained with these two methods, which we attribute to neglecting correlations present in Eq. (14) between T_c and the single-particle eigenfunctions in the kernel M and eigenvalues ϵ_m. Our correct numerical treatment of disorder clearly demonstrates the enhancement of the critical temperature in comparison to other mean-field approaches relying on neglecting the correlations in Eq. (14) for the critical temperature.

We observe that for strong enough couplings, the critical temperature is self-averaging; however, that breaks for weaker couplings. We introduced the quantity $\tilde{\lambda}$ to quantify the breakdown of the self-averaging property of the critical temperature. When $\lambda > \tilde{\lambda}$, the self-averaging is well preserved, and the distribution of the critical temperature can be approximated by a Gaussian. On the other hand, when $\lambda \leqslant \tilde{\lambda}$, the standard deviation starts to spread significantly, indicating that the solution for the critical temperature becomes extremely sensitive to the disorder realization.

Note added. Recently, we became aware of an interesting related work [46].

ACKNOWLEDGMENTS

T.Č., A.A. and M.S. acknowledge the financial support from the Institute for Basic Science (IBS) in the Republic of Korea through Project No. IBS-R024-D1. M.S. also want to acknowledge the financial support from Beijing Municipal Education Commission individually. I.Y. gratefully acknowledges support from the Leverhulme Trust under Grant No. RPG-2019-317. We thank A. Jagannathan for drawing our attention to Refs. [42,43].

[1] D. ben-Avraham and S. Havlin, *Diffusion and Reactions in Fractals and Disordered Systems* (Cambridge University Press, Cambridge, 2000).

[2] B. Mandelbrot, *Fractals: Form, Chance, and Dimension* (Echo Point Books and Media, Brattleboro, 2020).

[3] K. Zhao, H. Lin, X. Xiao, W. Huang, W. Yao, M. Yan, Y. Xing, Q. Zhang, Z.-X. Li, S. Hoshino, J. Wang, S. Zhou, L. Gu, M. S. Bahramy, H. Yao, N. Nagaosa, Q.-K. Xue, K. T. Law, X. Chen, and S.-H. Ji, Disorder-induced multifractal superconductivity in monolayer niobium dichalcogenides, Nat. Phys. **15**, 904 (2019).

[4] C. S. I. Y. Hyang, Y. M. Ju, and L. D. Yoon, Fractal solar cell array for enhanced energy production: Applying rules underlying tree shape to photovoltaics, Proc. R. Soc. A **476**, 20200094 (2020).

[5] B. Fazio, P. Artoni, M. A. Iatì, C. D'Andrea, M. J. Lo Faro, S. Del Sorbo, S. Pirotta, P. S. Gucciardi, P. Musumeci, C. S. Vasi, R. Saija, M. Galli, F. Priolo, and A. Irrera, Strongly enhanced light trapping in a two-dimensional silicon nanowire random fractal array, Light: Sci. Appl. **5**, e16062 (2016).

[6] J. Bardeen, L. N. Cooper, and J. R. Schrieffer, Microscopic theory of superconductivity, Phys. Rev. **106**, 162 (1957).

[7] J. Bardeen, L. N. Cooper, and J. R. Schrieffer, Theory of superconductivity, Phys. Rev. **108**, 1175 (1957).

[8] P. B. Allen and B. Mitrović, *Theory of Superconducting T_c* (Academic Press, Cambridge, Massachusetts, 1983), pp. 1–92.

[9] P. Anderson, Theory of dirty superconductors, J. Phys. Chem. Solids **11**, 26 (1959).

[10] M. Strongin, R. S. Thompson, O. F. Kammerer, and J. E. Crow, Destruction of superconductivity in disordered near-monolayer films, Phys. Rev. B **1**, 1078 (1970).

[11] Y. Imry and M. Strongin, Destruction of superconductivity in granular and highly disordered metals, Phys. Rev. B **24**, 6353 (1981).

[12] I. V. Yurkevich and I. V. Lerner, Nonlinear σ model for disordered superconductors, Phys. Rev. B **63**, 064522 (2001).

[13] I. Burmistrov, S. Bera, F. Evers, I. Gornyi, and A. Mirlin, Wave function multifractality and dephasing at metal–insulator and quantum Hall transitions, Ann. Phys. (NY) **326**, 1457 (2011).

[14] M. S. Foster, H.-Y. Xie, and Y.-Z. Chou, Topological protection, disorder, and interactions: Survival at the surface of three-dimensional topological superconductors, Phys. Rev. B **89**, 155140 (2014).

[15] M. Stosiek, B. Lang, and F. Evers, Self-consistent-field ensembles of disordered Hamiltonians: Efficient solver and

application to superconducting films, Phys. Rev. B **101**, 144503 (2020).
[16] V. I. Fal'ko and K. B. Efetov, Multifractality: Generic property of eigenstates of 2D disordered metals, Europhys. Lett. **32**, 627 (1995).
[17] M. V. Feigel'man, L. B. Ioffe, V. E. Kravtsov, and E. A. Yuzbashyan, Eigenfunction fractality and pseudogap state near the superconductor-insulator transition, Phys. Rev. Lett. **98**, 027001 (2007).
[18] M. Feigel'man, L. Ioffe, V. Kravtsov, and E. Cuevas, Fractal superconductivity near localization threshold, Ann. Phys. (NY) **325**, 1390 (2010).
[19] J. Mayoh and A. M. García-García, Global critical temperature in disordered superconductors with weak multifractality, Phys. Rev. B **92**, 174526 (2015).
[20] A. Lowe, V. Kagalovsky, and I. V. Yurkevich, Disorder-enhanced superconductivity in a quasi-one-dimensional strongly correlated system, Phys. Rev. Res. **3**, 033059 (2021).
[21] V. Kagalovsky, A. Lowe, D. Yurkevich, and I. Yurkevich, Disorder-induced phase transitions in a spinful one-dimensional system, Ann. Phys. (NY) **435**, 168482 (2021).
[22] X. Zhang and M. S. Foster, Enhanced amplitude for superconductivity due to spectrum-wide wave function criticality in quasiperiodic and power-law random hopping models, Phys. Rev. B **106**, L180503 (2022).
[23] Y. V. Fyodorov and A. D. Mirlin, Strong eigenfunction correlations near the Anderson-localization transition, Phys. Rev. B **55**, R16001 (1997).
[24] Y. Taguchi, A. Kitora, and Y. Iwasa, Increase in T_c upon reduction of doping in Li_xZrNCl superconductors, Phys. Rev. Lett., 97, 107001 (2006).
[25] V. E. Kravtsov, Wonderful life at weak Coulomb interaction: Increasing of superconducting/superfluid transition temperature by disorder, J. Phys.: Conf. Ser. **376**, 012003 (2012).
[26] S. Sakai, N. Takemori, A. Koga, and R. Arita, Superconductivity on a quasiperiodic lattice: Extended-to-localized crossover of Cooper pairs, Phys. Rev. B **95**, 024509 (2017).
[27] N. Takemori, R. Arita, and S. Sakai, Physical properties of weak-coupling quasiperiodic superconductors, Phys. Rev. B **102**, 115108 (2020).
[28] L. Yan and P. Liljeroth, Engineered electronic states in atomically precise artificial lattices and graphene nanoribbons, Adv. Phys.: X **4**, 1651672 (2019).
[29] A. Jagannathan, The Fibonacci quasicrystal: Case study of hidden dimensions and multifractality, Rev. Mod. Phys. **93**, 045001 (2021).
[30] C. Chiaracane, F. Pietracaprina, A. Purkayastha, and J. Goold, Quantum dynamics in the interacting Fibonacci chain, Phys. Rev. B **103**, 184205 (2021).
[31] N. Macé, N. Laflorencie, and F. Alet, Many-body localization in a quasiperiodic Fibonacci chain, SciPost Phys. **6**, 050 (2019).
[32] N. Macé, A. Jagannathan, and F. Piéchon, Fractal dimensions of wave functions and local spectral measures on the Fibonacci chain, Phys. Rev. B **93**, 205153 (2016).
[33] D. Tanese, E. Gurevich, F. Baboux, T. Jacqmin, A. Lemaître, E. Galopin, I. Sagnes, A. Amo, J. Bloch, and E. Akkermans, Fractal energy spectrum of a polariton gas in a Fibonacci quasiperiodic potential, Phys. Rev. Lett. **112**, 146404 (2014).
[34] F. Fang, An icosahedral quasicrystal as a golden modification of the icosagrid and its connection to the E8 lattice, Acta Cryst. Sect. A **71**, s417 (2015).
[35] K. Kamiya, T. Takeuchi, N. Kabeya, N. Wada, T. Ishimasa, A. Ochiai, K. Deguchi, K. Imura, and N. K. Sato, Discovery of superconductivity in quasicrystal, Nat. Commun. **9**, 154 (2018).
[36] M. Kohmoto, B. Sutherland, and C. Tang, Critical wave functions and a cantor-set spectrum of a one-dimensional quasicrystal model, Phys. Rev. B **35**, 1020 (1987).
[37] Q. Niu and F. Nori, Spectral splitting and wave-function scaling in quasicrystalline and hierarchical structures, Phys. Rev. B **42**, 10329 (1990).
[38] Z. Fan, G.-W. Chern, and S.-Z. Lin, Enhanced superconductivity in quasiperiodic crystals, Phys. Rev. Res. **3**, 023195 (2021).
[39] E. Cuevas and V. E. Kravtsov, Two-eigenfunction correlation in a multifractal metal and insulator, Phys. Rev. B **76**, 235119 (2007).
[40] J. Chalker, Scaling and eigenfunction correlations near a mobility edge, Physica A (Amsterdam, Neth.) **167**, 253 (1990).
[41] F. Evers and A. D. Mirlin, Anderson transitions, Rev. Mod. Phys. **80**, 1355 (2008).
[42] S. Thiem and M. Schreiber, Wavefunctions, quantum diffusion, and scaling exponents in golden-mean quasiperiodic tilings, J. Phys.: Condens. Matter **25**, 075503 (2013).
[43] A. Jagannathan and M. Tarzia, Electronic states of a disordered two-dimensional quasiperiodic tiling: From critical states to Anderson localization, Phys. Rev. B **107**, 054206 (2023).
[44] M. Ma and P. A. Lee, Localized superconductors, Phys. Rev. B **32**, 5658 (1985).
[45] G. D. Mahan, *Many-Particle Physics*, Physics of Solids and Liquids (Springer, New York, 2013).
[46] R. Oliveira, M. Gonalves, P. Ribeiro, E. V. Castro, and B. Amorim, Incommensurability-induced enhancement of superconductivity in one dimensional critical systems, arXiv:2303.17656.